JPEDAV (2005) 26:534-538
DOI: 10.1361/154770305X66682
1547-7037/$19.00 ©ASM International

The Influence of Diffusion on Hydrate Growth

Atle Svandal, Bjørn Kvamme, Làszlò Gràànàsy, and Tamàs Pusztai

(Submitted July 18, 2005)

In this study, we examine the rate-limiting process for the formation of hydrates from aqueous solutions of CO_2 and the rate-limiting process when CO_2 hydrate dissociates toward pure water. A phase field theory is applied to model the growth and dissociation of the gas hydrate in a system consisting of an aqueous CO_2 phase, and an initial hydrate nucleus at constant pressure of 150 bar and a temperature of 274.15 K. The diffusion of CO_2 in the aqueous phase is shown to be the governing parameter for the growth and dissociation rates. We investigate concentration profiles at the interface and show that diffusion through Fick's law in the liquid can account for the behavior of the system. We argue that the released heat has little or no effect on the kinetics of growth and dissociation for the systems in this study, although we cannot exclude the potential effect of released heat on the nucleation stage. Finally, we also discuss the effects of anisotropic crystal growth on crystal morphology and kinetic rates of growth.

1. Introduction

Gas hydrates are crystalline structures in which water forms cavities that enclathrate small nonpolar molecules, so-called *guest molecules*, such as CO_2 or CH_4. Macroscopically, the structure looks similar to ice or snow, but unlike ice these hydrates are also stable at temperatures above 0 °C. The enclathrated molecules stabilize the hydrate through their volume and their interactions with the water molecules that constitute the cavity walls. Hydrate can form and grow from aqueous solution of guest molecules if the pressure, temperature, and concentrations of these molecules are favorable. Historically, the importance of hydrates has been dominated by the industrial problems related to hydrocarbon hydrate formation in equipment and pipelines during processing and transport. During more recent years, the interest in hydrates has expanded in other directions. The total amount of energy related to hydrocarbons trapped in hydrates may be more than twice the amount of all known sources of coal and natural hydrocarbon sources. Historically, some of the hydrate reservoirs have experienced catastrophic dissociations. One example is the Storegga slide. The largest slide in this area was created 7000 years ago and induced a tsunami that drowned Scotland. The second largest gas field outside Norway is located in the Storegga region, and the installation of equipment in sediments containing hydrate as well as drilling though hydrate sediments is another important issue related to hydrate stability. The stability and kinetics of hydrate depends, as indicated, on temperature and pressure as well as on the concentrations of all the components involved in the phase transition. In the current study, the main focus is on growth of CO_2 hydrate from an aqueous solution and the dissociation of CO_2 hydrate when exposed to pure water. This type of system is important for the storage of CO_2 in cold aquifers. There are several regions around hydrocarbon fields with low seafloor temperatures and corresponding zones in the reservoir beneath that are inside the range of hydrate stability. The potential for the leakage of CO_2 from reservoirs in these regions may be reduced by the formation of a hydrate film on the interface between rising CO_2 plumes and groundwater. The kinetics and mechanisms of hydrate formation as well as hydrate dissociation toward pure water is essential to understand the potential leakage rates through the hydrate. Knowledge of the rate-limiting mechanisms for the kinetics will make it possible to establish simplified correlations that can be implemented in reservoir-modeling tools.

2. Phase Field Theory

A phase field theory has previously been applied to describe the formation of CO_2 hydrate in aqueous solutions.[1] Here, a similar version of the theory is applied to model the growth and dissociation of CO_2 hydrate. The solidification of the hydrate is described in terms of the scalar phase field ϕ and the local solute concentration c. The field ϕ is a structural order parameter assuming the values $\phi = 0$ in the solid and $\phi = 1$ in the liquid. Intermediate values correspond to the interface between the two phases. Only a short review of the model will be given here. Full details of the derivation and numerical methods can be found elsewhere.[1-4] The starting point is a free-energy functional:

$$F = \int dr^3 \left[\frac{1}{2}\varepsilon^2 T \left| \nabla\phi \right|^2 + f(\phi,c) \right] \quad \text{(Eq 1)}$$

where ε is a constant, T is the temperature, and the integration is over the system volume. The phase field literature contains some ambiguities when it comes to the use of the

This article is a revised version of the paper printed in the *Proceedings of the First International Conference on Diffusion in Solids and Liquids—DSL-2005*, Aveiro, Portugal, July 6-8, 2005, Andreas Öchsner, José Grácio, and Frédéric Barlat, Ed., University of Aveiro, 2005.

Atle Svandal and **Bjørn Kvamme,** Department of Physics and Technology, University of Bergen, Allègaten 55, N-5007 Bergen, Norway; and **Làszlò Gràànàsy** and **Tamàs Pusztai,** Research Institute for Solid State Physics and Optics, H-1525 Budapest, POB 49, Hungary. Contact e-mail: atle.svandal@ift.uib.no.

terms *concentration* and *mole fraction*. In this article, we use c for concentration with units of moles per volume, and the mole fraction of CO_2 is termed x and is dimensionless. Assuming equal molar volume for the two components, the relation $c = x/v_m$ can be applied, where v_m is the average molar volume. The range of the thermal fluctuations is on the order of the interfacial thickness, and, accordingly, ε may be fixed from knowledge of this thickness. The gradient term is a correction to the local free-energy density $f(\phi,c)$. To ensure the minimization of the free energy and the conservation of mass, the governing equations can be written as:

$$\dot{\phi} = -M_\phi \frac{\delta F}{\delta \phi} \quad \text{(Eq 2)}$$

$$\dot{c} = \nabla\left(M_c \nabla \frac{\delta F}{\delta c} \right) \quad \text{(Eq 3)}$$

where M_c and M_ϕ are the mobilities associated with a coarse-grained equation of motion, which in turn are related to their microscopic counterparts. To reproduce bulk fluid diffusion, $M_c = Dx(1 - x)/RT$, where $D = D_s + (D_l - D_s)p(\phi)$ is the diffusion coefficient with $D = 1.0 \times 10^{-9}$ m^2/s, the diffusion coefficient in the liquid,[5] and $D_s = 1.1 \times 10^{-12}$ m^2/s for the solid.[6] The local free-energy density is assumed to have the form:

$$f(\phi,c) = wTg(\phi) + [1 - p(\phi)]f_s(c) + p(\phi)f_L(c) \quad \text{(Eq 4)}$$

where the *double well* and *interpolation* functions have the forms $g(\phi) = 1/4\phi^2(1 - \phi)^2$ and $p(\phi) = \phi^3(10–15\phi + 6\phi^2)$, which emerge from the thermodynamically consistent formulation of the theory.[4] The parameter w is proportional to the interfacial free energy and can be deduced from experimental measurements[7] or predicted from molecular simulations of representative model systems.[8] Work along these lines is in progress[9] for the liquid water/hydrate interface. At the present moment, the applied value is 29.1 mJ/m^2.[7]

2.1 Fluid Thermodynamics

The free-energy density is calculated as:

$$v_m f_L = x \cdot g_{CO_2} + (1 - x)g_w \quad \text{(Eq 5)}$$

Here g_{CO_2} and g_w are the partial molar free energies of CO_2 and water, respectively. For the CO_2 we have:

$$g_{CO_2} = g^{\infty}_{CO_2}(T) + RT \ln(x\gamma_{CO_2}) \quad \text{(Eq 6)}$$

Here $g^{\infty}_{CO_2}(T)$ is the partial molar free energy at infinite dilution, which was found in molecular dynamics simulations, and for 274.15 K it is $g^{\infty}_{CO_2} = -19.67$ kJ/mole. R is the universal gas constant, and γ_{CO_2} is the activity coefficient of CO_2 in an aqueous solution in the asymmetric convention (γ_{CO2} is unity in the limit as x goes to 0) deduced from CO_2 solubility experiments and fitted to a logarithmic expansion in temperature.[1] For water, we have:

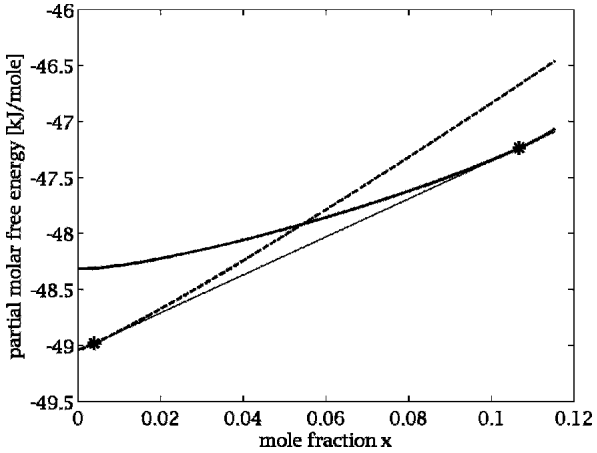

Fig. 1 Molar free energies of the different phases involved in the phase transitions as a function of the mole fraction of CO_2. Solid line, hydrate; dashed line, liquid; thin line, the common tangent

$$g_w = g^{pure}_w(T) + RT \ln[(1 - x)\gamma_w] \quad \text{(Eq 7)}$$

Here, $g^{pure}_w(T)$ is the partial molar free energy of pure water, and Ref 10 gives a value of 274.15 K for $g^{pure}_w = -49.31$ kJ/mole. The activity coefficient of water has been obtained through the Gibbs-Duhem relation.

2.2 Hydrate Thermodynamics

The thermodynamics of the hydrate is based on the model by Kvamme and Tanaka[10] and van der Waals and Platteeuw.[11] The free energy is, as for the liquid, calculated as:

$$v_m f_s = x \cdot g^H_{CO_2} + (1 - x)g^H_w \quad \text{(Eq 8)}$$

The expressions for the partial molar free energies for water and CO_2 in hydrate are:

$$g^H_{CO_2} = \Delta g^{inc} + RT \ln\left(\frac{\theta}{1 - \theta} \right) \quad \text{(Eq 9)}$$

$$g^H_w = g^{0,H}_w + RTv_L \ln(1 - \theta) \quad \text{(Eq 10)}$$

The filling fraction of large cavities is given as $\theta = x/[v_L(1 - x)]$. From Ref 10, the values of pure hydrate and partial molar inclusion of CO_2 at 274.15 K are $g^{0,H}_w = -48.46$ kJ/mole and $\Delta g^{inc} = -37.52$ kJ/mole.

2.3 Saturation and Equilibrium

Figure 1 shows the total molar free energies for solid and liquid as a function of the filling fraction. The coexistence point between the two phases can be calculated by the common-tangent method. The same results can be obtained by solving the equations for the equal chemical potential of each component in the two phases. The common tangent points thus correspond to the equilibrium mole fractions of each phase.

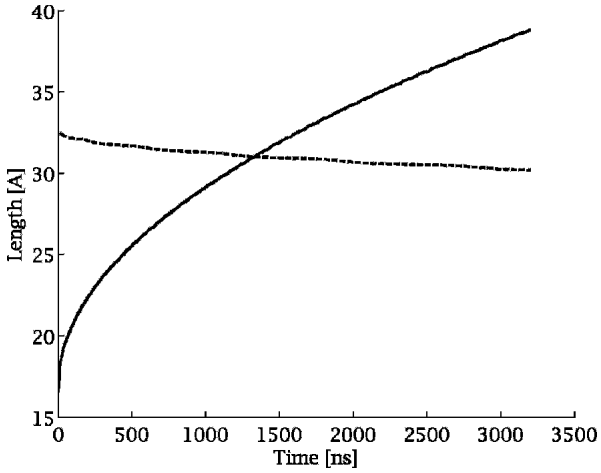

Fig. 2 Position of the front as a function of time for the dissociation and growth simulation. Solid line, growth; dashed line, dissociation

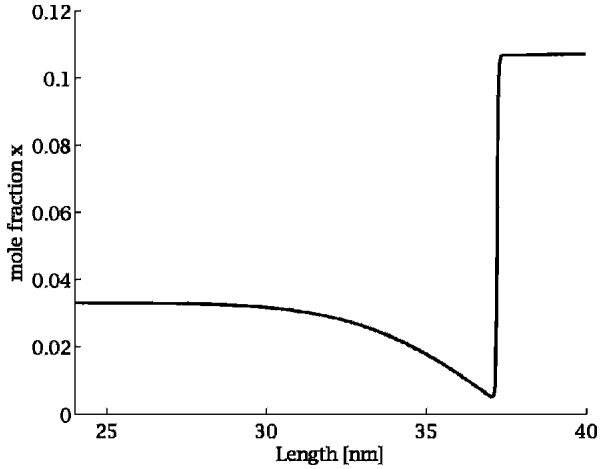

Fig. 3 Concentration profile of the interface under growing conditions after 1 μs

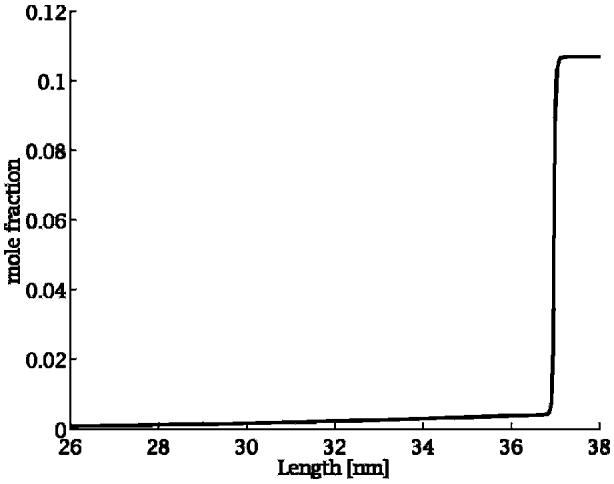

Fig. 4 Concentration profile of the interface under dissociation conditions after 1 μs

The mole fraction in the water under equilibrium is $x_a = 4.02 \times 10^{-3}$, and for the hydrate $x_h = 0.107$, which is marked by asterisks in Fig. 1. This defines the stability region in terms of the mole fractions. Hydrate exposed to water within areas of stability with respect to temperature and pressure, with a higher mole fraction than x_a, will grow. Hydrate under the same condition but exposed to water with a lower mole fraction than x_a will melt.

3. Hydrate Growth and Dissociation

3.1 Numerical Results

The model has been implemented on a 1000 × 10 grid to simulate growth and the dissociation of a planar surface, assuming fluxless boundary conditions at the walls. Pressure and temperature are assumed to remain constant in the system at 150 bars and 274.15 K, respectively. The grid resolution is 4 Å, and the time step is 1.6×10^{-12} s. Initially, we started with a supersaturated CO_2-water solution and a hydrate film with a thickness of 16 nm for the growth simulation, and a 32 nm thick hydrate film exposed to pure water in the dissociation simulation. The supersaturated solution is $x_s = 0.033$ representing the meta-stable equilibrium between water and liquid-CO_2.[12] The movement of the front is tracked by following the $\phi = 0.5$ value, and the results are plotted in Fig. 2.

The interface under both simulations follows perfectly a power law, $\propto t^{1/2}$, already indicating a diffusion-controlled process. A square root function can be fitted to interpolate interface velocities at experimental time scales. After 1*s*, the growth rate following this function will be $v(1s) = 6$ μm/s, which is comparable to the experimental results. Further discussion on this number is found in section 3.4.

3.2 Concentration Profiles

To investigate further the diffusion dependence, we take a closer look at the concentration profile near the interface seen in Fig. 3 and 4.

To the far left in both figures, the mole fraction equals the initial values; the CO_2 has not yet diffused to or from these regions. At the interface, minima very rapidly evolve for the growth simulation approximately at the hydrate equilibrium value x_a. For the dissociation simulation, the mole fraction in the solution approaches the x_a limit on the interface. The kinetics can be viewed as a moving local equilibrium interface where the velocity is determined by the transport of CO_2 toward or away from this interface. From the simulations, we can calculate an effective flux using a Fick's law approach in which the concentration gradient in the solution is used. According to Fick's law, the flux can be calculated as:

$$J = -D\frac{\Delta c}{\Delta x} \qquad \text{(Eq 11)}$$

Taking the gradient close to the minima but in the liquid, a velocity of the interface that is comparable to the simulated velocity is obtained. The result is shown in Fig. 5.

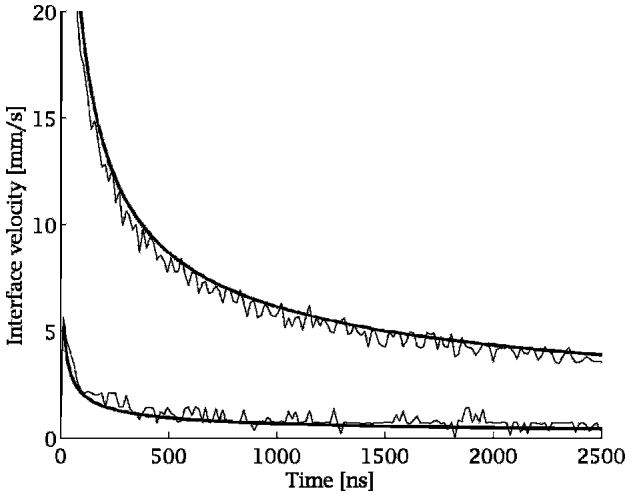

Fig. 5 Absolute value of the interface velocity for the growth and dissociation simulation. Upper thick line, growth velocity; lower thick line, dissociation velocity; thin lines, the calculated velocities

The noise on the calculated curve is due to grid effects. These results seem to be able to account for the process of hydrate growth and dissociation (i.e., the limiting process for dissociation of the hydrate is the transport of CO_2 away from the interface), and likewise the growth is limited by the transport toward the interface. There are three terms in the expression for the flux in Eq 11. The diffusion coefficient D_l in the solution is not dependent on the mole fraction, and we can also assume that the characteristic length Δx is the same for growth and dissociation. The difference in the concentration between the initial condition and the saturated x_a can be taken as the Δc term and will determine the flux. If the growth and dissociation scenarios are compared, growth will be $\Delta c \propto x_s - x_a$, and dissociation $\Delta c \propto x_a - 0$. Because $x_s > x_a$, with about one order of magnitude, the growth rate should be larger than the dissociation rate; the results from Fig. 5 show that this is a good relation giving a difference in interface velocity by the same order of magnitude. For the growth or dissociation of hydrate exposed to an aqueous solution of CO_2 and water, the most important parameter then would seem to be the initial fraction of CO_2 in the solution. Other parameters such as changes in driving force due to temperature or pressure changes are less important.

3.3 Temperature

The assumption of isothermal phase transition for the systems in this study is based on the relative magnitude of the thermal conductivity compared with mass diffusivity. Some rough estimates can be made if we assume that the heat released through hydrate formation is converted into sensible heat according to Fourier's law. Our simulations are two-dimensional, and if we assume that the growth is homogeneous in the direction perpendicular to the hydrate plane z, we may write:

$$\frac{\partial T}{\partial z} = v_z \frac{\rho^H \Delta H}{k} \approx v_z \cdot 5.5 \times 10^{-7} \frac{K}{m} \qquad \text{(Eq 12)}$$

where v_z is the hydrate growth velocity in the z direction, and the approximate relationship on the right-hand side is based on the following numbers and assumptions. The term ρ^H is the molar density of the hydrate, which for complete filling is 49,809 mol/m^3. The term ΔH is the enthalpy of the hydrate formation, which is trivially calculated from the corresponding free energies of hydrate formation through standard thermodynamic relationships. The estimated value is 604 J/mole under the actual conditions, and k is the thermal conductivity. The thermal conductivity of liquid water is 0.55 W/m · K at 1 °C. The value of the thermal conductivity of hydrate is similar in value. If the hydrate film is on the interface between liquid CO_2 and the aqueous phase, we may approximately assume heat flux only into the aqueous phase due to the low heat conductivity of CO_2. From the simulated results plotted in Fig. 2, the growth rate decays from 6 mm/s after 1 μs to 0.006 mm/s after 1 s. Within the approximate nature of these estimates, the temperature change during the first 4 nm of hydrate growth is thus $<10^{-16}$ K and is even relatively smaller for subsequent stages of growth. The assumption of isothermal phase transitions for the systems presented in this study is therefore considered to be appropriate.

3.4 Anisotropy

In contrast to isotropic growth in which the two model parameters ε and w are fixed through information on the interfacial properties, there is no similar theoretical relationship to relate anisotropic crystal growth. On the other hand, at the cost of a few empiric model parameters the phase field approach has been proven[2,3] to be able to reproduce the growth of many experimentally observed crystal structures. The relative impact of these orientation effects on kinetic growth rates and kinetic-limiting contributions is an important issue. For this purpose, Eq 1 is extended with an oriental field,[2] and the constant ε is assumed to be directionally dependent and is expressed as:

$$\varepsilon \rightarrow \varepsilon' \left[1 + \frac{s_0}{2} \cos(n\partial - 2\pi\theta) \right] \qquad \text{(Eq 13)}$$

Herein s_0 is the anisotropic amplitude, n is the symmetry, θ is the introduced orientation field, and $\partial = \arctan[(\nabla\phi)_y/(\nabla\phi)_x]$. The running of the anisotropic simulation result in a dendritic structure is shown in Fig. 6.

The interface velocity for dendritic growth should theoretically approach a constant value. The results from our anisotropic simulations yield a faster growth rate than the isotropic simulation, deviating more and more from a square root law as the system evolves. The simulations are unfortunately computationally expensive, and we have not yet been able to achieve such convergence.

4. Conclusions

According to the results obtained from phase field simulations in this study, the growth and dissociation of CO_2 hydrates are shown to be governed by the diffusion of CO_2 in the aqueous phase. The most important parameters when

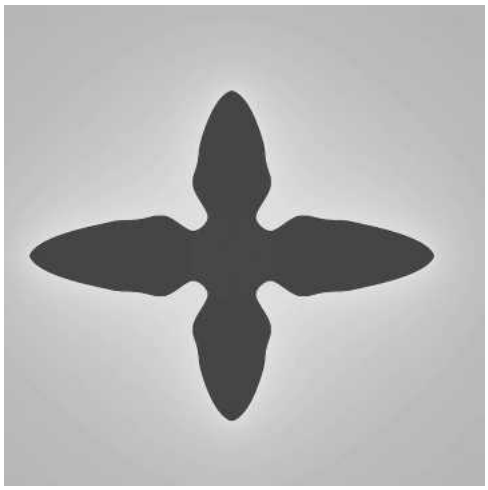

Fig. 6 Anisotropic growth of hydrate

it comes to the growth and dissociation rate will be the initial mole fraction of CO_2 in the aqueous phase. This result gives us a simple and valuable qualitative understanding of the process that should be taken into account when quantities such as the growth and dissociation rates are measured in experimental setups. These processes are also of particular interest relative to the storage of CO_2 in cold aquifers where the formation of a hydrate film might induce extra stabilization to the CO_2 in storage. The CO_2 leakage will then be determined by the dissociation of the hydrate film.

Acknowledgments

The authors wish to thank Trygve Buanes and Joakim Hove for fruitful discussions. Financial support from the Norwegian Research Council through project 101204, and from Conoco-Phillips, is highly appreciated.

References

1. B. Kvamme, G. Graue, E. Aspenes, T. Kuznetsova, L. Grànàsy, G. Tòth, T. Pusztai, and G. Tegze, Kinetics of Solid Hydrate Formation by Carbon Dioxide: Phase Field Theory of Hydrate Nucleation and Magnetic Resonance Imaging. *Phys. Chem. Chem. Phys.,* Vol 6, 2004, p 2327-2334
2. L. Grànàsy, T. Börzsönyi, and T. Pusztai, Nucleation and Bulk Crystallization in Binary Phase Field Theory, *Phys. Rev. Lett.,* Vol 88, 2002, 206105 p 1-4
3. J.A. Warren and W.J. Boettinger, Prediction of Dendritic Growth and Microsegragation Patterns in a Binary Alloy Using the Phase-Field Method, *Acta Metall. Mater.,* Vol 43, 1995, p 689-703
4. S.L. Wang, R.F. Sekerka, A.A. Wheeler, B.T. Murray, S.R. Coriell, R.J. Braun, and G.B. McFadden, Thermodynamically-Consistent Phase-Field Models for Solidification, *Physica D,* Vol 69, 1993, p 189-200
5. G. Rehder, S.H. Kirby, W.B. Durham, L.A. Stern, E.T. Peltzer, J. Pinkston, and P.G. Brewer, Dissolution Rates of Pure Methane Hydrate and Carbon-Dioxide Hydrate in Undersaturated Seawater at 1000-m Depth. *Geochim. Cosmochim. Acta,* Vol 68, 2004, p 285-292
6. R. Radhakrishnan, A. Demurov, H. Herzog, and B.L. Trout, A Consistent and Verifiable Macroscopic Model for the Dissolution of Liquid CO_2 in Water Under Hydrate Forming Conditions, *Energy Conv. Manag.,* Vol 44, 2003, p 771-780
7. S.C. Hardy, A Grain Boundary Groove Measurement of the Surface Tension between Ice and Water. *Philos. Mag.,* Vol 35, 1977, p 471
8. R.L. Davidchack and B.B. Laird, Simulation of the Hard-Sphere Crystal-Melt Interface. *J. Chem. Phys.,* Vol 108, 1998, p 9452-9462
9. T. Kuznetsova and B. Kvamme, Predictions of Interfacial Free Energies from Molecular Dynamics Simulations. unpublished data, 2005
10. B. Kvamme and H. Tanaka, Thermodynamic Stability of Hydrates for Ethane, Ethylene, and Carbon Dioxide. *J. Phys. Chem.,* Vol 99, 1995, p 7114-7119
11. J.H. van der Waals and J.C. Platteeuw, Clathrate Solutions, *Adv. Chem. Phys.,* Vol 2, 1959, p 1-57
12. L.W. Diamond and N.N. Akinfiev, Solubility of CO_2 in Water From −1.5 to 100 °C and From 0.1 to 100 MPa: Evaluation of Literature Data and Thermodynamic Modelling. *Fluid Phase Equilib.,* Vol 208, 2003, p 265-290